ISSN 1063-7761, Journal of Experimental and Theoretical Physics, 2008, Vol. 107, No. 1, pp. 126–132. © Pleiades Publishing, Inc., 2008.
Original Russian Text © A.S. Fedorov, M.V. Serzhantova, A.A. Kuzubov, 2008, published in Zhurnal Éksperimental'noĭ i Teoreticheskoĭ Fiziki, 2008, Vol. 134, No. 1, pp. 156–163.

ELECTRONIC PROPERTIES OF SOLIDS

Analysis of Hydrogen Adsorption in the Bulk and on the Surface of Magnesium Nanoparticles

A. S. Fedorov[a], M. V. Serzhantova[b], and A. A. Kuzubov[a,b]

[a] *Kirenskii Institute of Physics, Siberian Branch, Russian Academy of Sciences, Akademgorodok, Krasnoyarsk, 660036 Russia*

[b] *Siberian Federal University, Akademgorodok, Krasnoyarsk, 660028 Russia*

e-mail: alex06@akadem.ru

Received December 24, 2007

Abstract—The stability of magnesium hydride (MgH_x) nanoparticles ($x = 0.5, \ldots, 2$) is investigated using ab initio calculations. It is shown that for a nanoparticle diameter of $D \sim 5$ nm, the internal pressure becomes lower than 3 kbar; for this reason, the structure of hydride nanoparticles coincides with the structure of this hydride in crystalline form. It is found that the phase of partly saturated MgH_x hydrides ($x < 2$) must decompose into the phase of pure hcp magnesium and the α phase of MgH_2. The frequencies of jumps of hydrogen atoms within the hcp phase of magnesium and in the α phase of MgH_2 are calculated; it is shown that slow diffusion of hydrogen in magnesium is due to the large height of potential barriers for motion of hydrogen within MgH_2. To attain high diffusion rates, the structures of $Mg_{53}Sc$ and $Mg_{53}Ti$ crystals and their hydrides are calculated. It is found that the frequency of jumps of H atoms in $Mg_{53}ScH_{108}$ near the Sc atoms does not noticeably change as compared to the frequency of jumps in the α phase of MgH_2, while the frequency of jumps in $Mg_{53}TiH_{108}$ near Ti atoms is higher by approximately a factor of 2.5×10^6. This means that diffusion in manganese hydride with small admixtures of titanium atoms must be considerably eased. Chemical dissociation of hydrogen molecules on the (0001) surface of hcp magnesium, on the given surface with adjoined individual Ti atoms, and on the surface of a one-layer titanium cluster on the given surface of magnesium is investigated. It is found that dissociation of hydrogen at solitary titanium atoms, as well as on the surface of a Ti cluster, is facilitated to a considerable extent as compared to pure magnesium. This should also sharply increase the hydrogen adsorption rate in magnesium nanoparticles.

PACS numbers: 61.46.Hk, 61.50.Ah, 66.30.Ny

DOI: 10.1134/S1063776108070121

1. INTRODUCTION

One of the main problems in rapidly developing hydrogen power engineering is storage of hydrogen. A promising trend is the use of new complex metal hydrides (including their nanocluster form) as accumulators of hydrogen.

Magnesium is a suitable metal for sorption of hydrogen in view of its low atomic weight, low cost, availability, low toxicity, and (most importantly) the high weight content of hydrogen in magnesium hydride. The available experimental data [1, 2] show that magnesium forms the hydride MgH_2, in which the mass content of hydrogen is 7.6%, which satisfies generally accepted criteria for the use of hydrogen accumulators in automobiles (the requirement of the US Department of Energy (DOE) is 6.5 wt %). However, the low rate of hydrogen sorption and desorption processes rules out the use of magnesium for accumulating hydrogen. Experimental data show that the low diffusion rate for hydrogen atoms in the crystal lattice of magnesium is one reason for the low absorption rate of hydrogen. The absorption of hydrogen in the crystal structure is hampered by lattice dilatation, leading to accumulation of defects and sample cracking.

These problems can be solved using nanoparticles instead of a bulk material. The rate of saturation with hydrogen must increase, and cracking of a nanoparticle must be eliminated in this case. The determination of the geometry and other properties of such nanoparticles is a complicated problem. One of the methods for studying nanoparticles involves quantum-chemical analysis. In many cases, such analysis makes it possible to skip expensive experiments without deteriorating the reliability of results. Modern quantum-chemistry methods based on the ideology of density functional theory make it possible to theoretically study periodic crystals and the properties of surfaces and to simulate the properties of nanoparticles to a high degree of accuracy.

In this study, we will first determine the most stable phase of magnesium hydride (MgH_2) nanoparticles. Most materials are known to change their properties upon a transition to the nanosize range (e.g., the catalytic and sorption ability of nanoparticles qualitatively

change). In such changes, the large specific surface of a nanoparticle plays the most important role, necessitating analysis of the surface energy and induced pressure in the bulk of a particle. As a result, the phase state of small nanoparticles may substantially differ from the phase state of the substance in the form of an equilibrium macroscopic crystal. Thus, to correctly predict the structure of nanoparticles, we must know their specific surface energy, which determines the internal pressure and, hence, the phase state of nanoparticles. In searching for the most stable phase of MgH_2 nanoparticles, we calculated various phases of MgH_2 under different pressures.

One of the reasons for the low hydrogen absorption rate in magnesium is hampered by slow chemical dissociation of hydrogen on the surface of a particle due to low catalytic activity of the metal. This problem can be solved by implanting transition metal atoms, which are catalysts of dissociation of H_2 molecules, into the magnesium lattice. In [3], the Mg_7TiH_x cubic crystal phase ($x \approx 12.7$) with a hydrogen concentration of about 5.5 wt % was obtained by mixing MgH_2 and $TiH_{1.9}$ powders under a pressure of 8 GPa at a temperature of 873 K. Thermal properties of this compound were studied using programmed thermal desorption (PTD). It was found that this compound decomposes into Mg and $TiH_{1.9}$, releasing 4.7% of hydrogen at $T = 605$ K, which is 130 and 220 K lower than the desorption temperature for MgH_2 and $TiH_{1.9}$, respectively. This indicates that the hydrogen–metal bond in this hydride is weaker than in MgH_2 and $TiH_{1.9}$. Unfortunately, experiments show that this hydride, as well as triple hydrides such as $NaAlH_4$, decomposes into the initial components during dehydrogenization. For this reason, we study here the crystalline phase of a dilute alloy $Mg_{53}Ti$ and its hydride.

2. METHODS AND OBJECTS OF INVESTIGATION

All calculations were performed within density functional theory (DFT) with gradient corrections using the Vienna ab-initio simulation package (VASP) [6–8]. This program for ab initio calculations utilizes the pseudopotential and decomposition of wave functions in the basis of plane waves. To effectively reduce the number of basis functions and to save computation time, Vanderbilt ultrasoft pseudopotentials were used in this program for all atoms [9].

First of all, we analyzed the effect of magnesium particle size on the Laplace pressure in the particle. This pressure is associated with the tendency of the particle to minimize its surface due to the presence of surface energy. To analyze the effect of magnesium nanoparticle size on the stability of its hydride, pressure P in the nanoparticle was calculated for various sizes of the particle.

We first calculated for this purpose the binding energy E_{bulk} of the most stable (hcp) structure of magnesium at zero pressure, from which we calculated the binding energy per atom, $E_0 = E_{bulk}/N$, where N is the number of atoms in the bulk of the magnesium crystal cell being analyzed. Then we calculated specific surface energy E_{surf} for the (0001) surface of hcp magnesium. For this, we used a periodic metallic slab consisting of $5 \times 5 \times 3$ unit cells and having a cross-sectional area of 6.42×6.42 Å^2 and a thickness of about 31.68 Å; identical slabs were separated by a vacuum gap of about 10 Å. After the calculation of total binding energy E_{slab} of the slab, specific surface energy E_{surf} was determined using the expression

$$E_{surf} = \frac{E_{slab} - NE_0}{2S}, \quad (1)$$

where S is the area of one side of the slab surface. Surface energy E_{surf} calculated for this face was 0.27 eV/surface atom, which is in good agreement with the experimental value (see [10]). In this way, we calculated the specific surface energies for slabs with various orientations of the facets. According to the results, mean surface energy $\langle E_{surf} \rangle$ of a nanoparticle was determined by averaging the surface energies of various facets and using the variational minimum condition for surface energy. According to this condition, the areas of the surfaces of various faces of a nanoparticle must be inversely proportional to their surface energy (see [11, 12]).

Using the above relations and the calculated values of specific energy for various faces, we obtained the equilibrium shape of nanoparticles with various diameters, which was close to spherical judging from the mean value of the radius in various directions. Taking into account this result and using the equilibrium condition for a nanoparticle upon a change in its volume, we can easily derive the formula connecting pressure P in the bulk of the nanoparticle and its radius R:

$$P = \frac{2\langle E_{surf} \rangle}{R}. \quad (2)$$

Figure 1 shows the dependence of pressure in a Mg nanoparticle on its radius, which was calculated using this formula. This dependence shows that for nanoparticles with a radius $R > 5$ nm, the internal pressure is lower than 3 kbar. For such nanoparticles, we can use the results of calculations applicable to crystals under a pressure $P < 3$ kbar since such calculations can be carried out much more easily as compared to those for nanoparticles in view of periodicity of the lattice and the small size of the unit cell.

We also calculated the energies of formation of magnesium hydrides partly saturated with hydrogen and having the composition Mg_2H_x ($x = 1, 2, 2.5, 3, 3.5$). Since the crystal structures of these phases are not known from experiments, the structures of all experimentally known phases of completely saturated

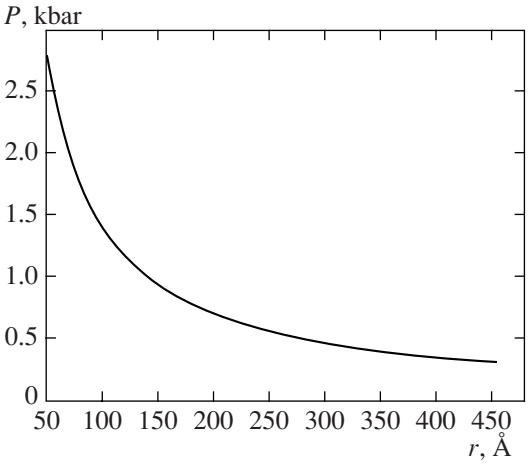

Fig. 1. Dependence of pressure in a Mg nanoparticle on its radius.

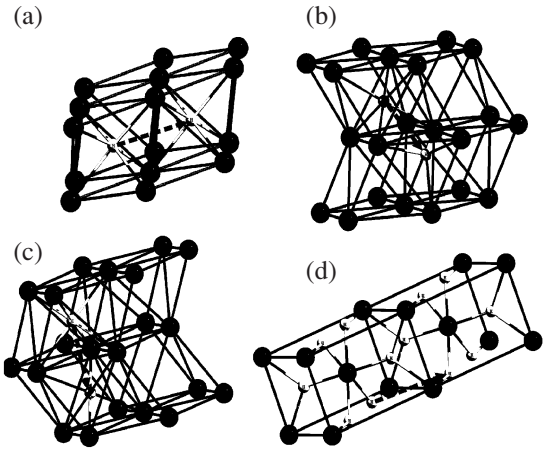

Fig. 2. Trajectories of jumps of hydrogen atoms in the hcp structure of Mg; (a) octahedron–octahedron; (b) octahedron–tetrahedron; (c) octahedron–octahedron in another configuration; (d) α phase of MgH_2.

Mg_2H_4 hydride were used as initial phases, into which hydrogen vacancies could be introduced. It is known from [2, 13] that crystalline magnesium hydride can form several phases depending on the external pressure, viz., the main α-MgH_2 phase existing under standard conditions, and phases β-MgH_2, γ-MgH_2, δ-MgH_2, and ε-MgH_2 which are stable at high temperatures and pressures. To calculate the binding energy, various numbers of hydrogen vacancies were introduced into all phases of MgH_2 (Table 1) and the phase having the minimal binding energy was chosen as the most stable phase.

Even rows in Tables 1 and 2 contain the results of calculations of binding energy (i.e., the values of enthalpy for $T, P = 0$) for all partly hydrogenated phases of hydrides MgH_x with vacancies. Odd rows contain weighted sums of enthalpies for pure magnesium and hydride MgH_2 in the corresponding phase taking into account their ratio per formula unit.

The data presented in the tables indicate that the enthalpies of all phases of hydrides Mg_2H_x (x = 1, 2, 2.5, 3, 3.5) with vacancies are much higher than the enthalpy for the weighted average of phases of pure magnesium and hydride MgH_2 in the α phase. This means that all partly hydrogenated hydrides must decompose into the sum of these two phases; in other words, spinodal decomposition must take place.

Table 1. Comparison of the binding energies for Mg_2H_x (x = 1–3) in the α phase and for weighed mean from the mixture of phases of pure hcp magnesium and Mg_2H_4 in the α phase

Hydrogen concentration		Binding energy, eV
Mg_2H_3	$Mg_2 + 3Mg_2H_4$	–56.282
	$4Mg_2H_3$	–52.589
Mg_2H_2	$Mg_2 + Mg_2H_4$	–20.798
	$2Mg_2H_2$	–19.919
Mg_2H	$3Mg_2 + Mg_2H_4$	–26.91
	$4Mg_2H$	–24.986

Using the nudge elastic band (NEB) method [14], we calculated the potential barriers to motion of a hydrogen atom in the crystal lattice between nearest potential energy minima. This method enables us, knowing the positions of the nearest energy minima of a moving particle, to calculate the reaction path (to find the trajectory of the particle minimizing the total energy at each point during its motion from one minimum to a neighboring one via the saddle point). For this purpose, it is as if two extreme positions of the particle at the energy minima are connected by an elastic band; minimizing the length of this band by varying its intermediate point, we can find the reaction path and the position of the saddle point.

Since hydrogen atoms can occupy both octahedral and tetrahedral holes in the structure of magnesium, the heights of the potential barriers for jumps between the nearest octahedron–octahedron pairs for two different configurations, as well as for the octahedron–tetrahedron jumps, were calculated using the above-mentioned method (see Figs. 2 and 3). Figure 2d and curve *4* in Fig. 3 show the potential barrier for jumps of a hydrogen atom between filled and empty positions in the α phase of MgH_2. Then we calculated the frequencies of jumps of a hydrogen atom at T = 300 K in all cases (specified in the caption to Fig. 3).

The calculated values of jump frequencies indicate an obvious reason for slow migration of H atoms in hydrides. Since it is advantageous for partly filled magnesium hydrides to decompose into the phases of pure magnesium and hydride MgH_2, the hydrogen diffusion rate is determined by its value in the α phase of hydride MgH_2, in which this value is low.

Table 2. Comparison of the binding energies for the β, γ, δ, and ε phases of Mg_4H_x (x = 1–3) and for weighed mean from the mixture of hcp magnesium and Mg_2H_4 in the α phase β, γ, δ, and ε phases of Mg_4H_8

Hydrogen concentration		Binding energy, eV			
		β-Mg_4H_8	γ-Mg_4H_8	δ-Mg_4H_8	ε-Mg_4H_8
Mg_4H_7	$2Mg_2 + 7Mg_4H_8$	–251.33	–254.32	–251.27	–246.24
	$8Mg_4H_7$	–244.73	–246.15	–244.64	–241.42
Mg_4H_6	$2Mg_2 + 3Mg_4H_8$	–111.21	–112.49	–111.18	–109.03
	$4Mg_4H_6$	–108.00	–108.02	–108.01	–108.36
Mg_4H_5	$6Mg_2 + 5Mg_4H_8$	–193.49	–195.63	–193.45	–189.86
	$8Mg_4H_5$	–185.59	–185.59	–185.61	–186.24
Mg_4H_4	$2Mg_2 + Mg_4H_8$	–41.14	–41.57	–41.13	–40.42
	$2Mg_4H_4$	–39.85	–39.84	–39.84	–40.07
Mg_4H_3	$10Mg_2 + 3Mg_4H_8$	–135.65	–136.94	–135.63	–133.47
	$8Mg_4H_3$	–129.58	–129.59	–129.57	–129.74
Mg_4H_2	$6Mg_2 + Mg_4H_8$	–53.37	–53.79	–53.36	–52.64
	$4Mg_4H_2$	–51.67	–51.67	–51.70	–51.52
Mg_4H	$14Mg_2 + Mg_4H_8$	–77.82	–78.24	–77.81	–77.09
	$8Mg_4H$	–75.09	–75.09	–74.95	–74.93

To solve the problem of the low rate of hydrogen adsorption in magnesium, we calculated the structure of dilute substitutional solution $Mg_{53}Sc$ and $Mg_{53}Ti$. Substituent Sc and Ti atoms were chosen because these metals have atomic radii close to the radius of magnesium, crystal lattices of the same type and, hence, may form substitution solutions with magnesium. In addition, the atoms of selected metals contain unpaired *d* electrons. Owing to the presence of a localized *d* electron, chemical dissociation of hydrogen molecules on the crystal surface must be substantially facilitated, which is indicated in experimental data (see [15]).

We then calculated the jump frequency for hydrogen in hydrides of corresponding alloys having compositions $Mg_{53}ScH_{108}$ and $Mg_{53}TiH_{108}$ in the α phase near the Sc and Ti atoms. For this purpose, a hydrogen vacancy in the vicinity of Sc or Ti atoms was introduced and the height of the potential barrier for a jump of a hydrogen atom from a filled position to such a vacancy was calculated. It was found that the height of this barrier in the vicinity of a Ti atom was approximately 0.4 eV lower that the height of the barrier in the α phase of MgH_2. At the same time, the height of the potential barrier for an analogous jump of hydrogen in the vicinity of a Sc atom is almost the same as for pure MgH_2 and is not shown in the figure. It follows hence that the hydrogen diffusion rate in the Mg_xTi_y alloy must be much higher than the diffusion rate in pure magnesium, Thus, the factor associated with complicated dissociation of hydrogen molecules on the magnesium surface can be overcome in view of its low catalytic activity.

To analyze the effect of Ti atoms on hydrogen dissociation more exactly, we simulated modification on the surface of magnesium by titanium atoms. The simulation was carried out in several stages. At the first stage, taking into account a solitary Ti atom on the magnesium surface, we calculated the energy of a slab consist-

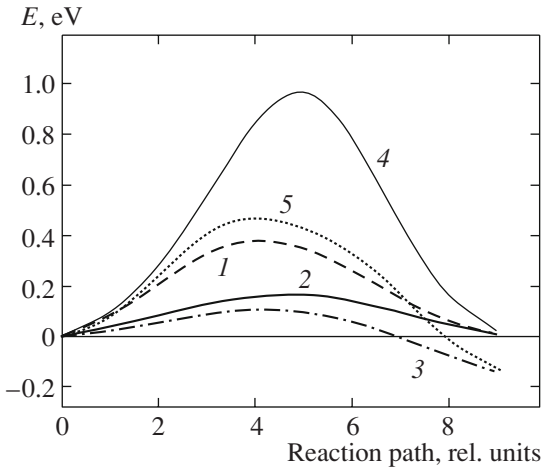

Fig. 3. Potential barriers for jumps of hydrogen atoms: *1*—octahedron–octahedron, *2*—octahedron–tetrahedron, *3*—octahedron–octahedron in another configuration; *4*—α phase of MgH_2; *5*—barrier for a jump of the hydrogen atom in the α phase of MgH_2 in the vicinity of a Ti atom. The rates of hydrogen jumps at T = 300 K for curves *1–5* are 9.21×10^8, 1.41×10^9, 1.63×10^{10}, 1.1×10^{-2}, and 2.70×10^4 s^{-1}, respectively.

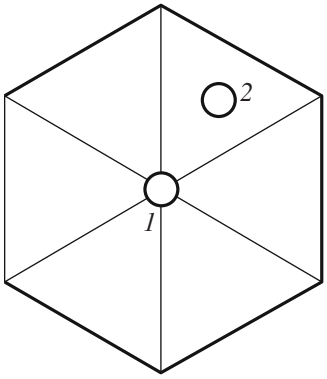

Fig. 4. Versions of arrangement of Ti atoms on the (0001) surface of the hexagonal structure of magnesium: *1*—Ti atom lies immediately above a Mg surface atom; *2*—Ti atom is between Mg atoms.

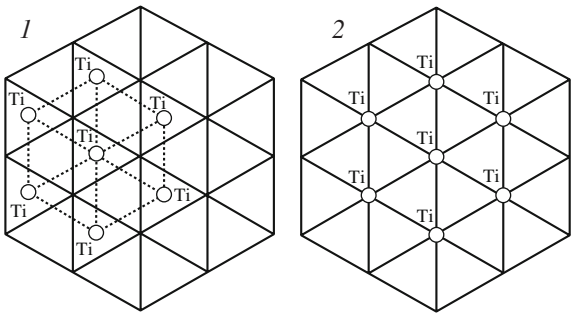

Fig. 5. Versions of arrangement of seven Ti atoms on the (0001) surface of the magnesium slab: *1*—Ti atoms are between Mg atoms without a violation of the hexagonal structure; *2*—Ti atoms are immediately above Mg atoms.

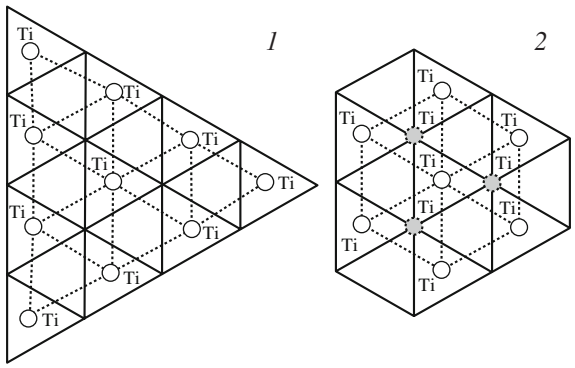

Fig. 6. Versions of arrangement of ten Ti atoms on the (0001) surface of the magnesium slab: *1*—one-layer titanium cluster; *2*—titanium cluster consisting of two layers (hatched circles correspond to Ti atoms in the second layer).

ing of 150 magnesium atoms ($3 \times 3 \times 3$ size of the unit cell surface) with the (0001) direction of the surface and with the energy of a single titanium atom. To find the minimal energy of binding of a titanium atom to the magnesium surface, we considered two cases: (i) the Ti atom lies immediately above the surface Mg atom; (ii) the Ti atom is at the center between two Mg atoms (see Fig. 4).

The Mg–Ti binding energy was calculated by the formula

$$E_{\text{Mg–Ti}} = E_{\text{Mg}_{150}\text{Ti}} - E_{\text{Mg}_{150}} - E_{\text{Ti}}, \quad (3)$$

where $E_{\text{Mg}_{150}\text{Ti}}$ is the binding energy of the magnesium surface with a Ti atom above it, $E_{\text{Mg}_{150}}$ is the binding energy of the magnesium slab, and E_{Ti} is the total energy of a single Ti atom. The binding energy corresponding to the first position is –4.579 eV, while the energy corresponding to the second position is –4.565 eV. Owing to the insignificant difference between these quantities, we can conclude that these two positions are almost equivalent.

The next step was the calculation of the binding energy between Ti atoms during the formation of an isolated one-layer cluster formed by these atoms on the surface of an analogous magnesium slab (see Figs. 5 and 6). In our calculations, seven Ti atoms were positioned above the slab in two different ways (see Fig. 5). In this case, the binding energy $E_{\text{Ti–Ti}}$ per atom was calculated by the formula

$$E_{\text{Ti–Ti}} = \frac{1}{7}(E_{\text{Mg}_{150}\text{Ti}_7} - E_{\text{Mg}_{150}} - 7E_{\text{Ti}} - 7E_{\text{Mg–Ti}}), \quad (4)$$

where $E_{\text{Mg}_{150}\text{Ti}_7}$ is the total binding energy of the magnesium slab with the Ti cluster, $E_{\text{Mg}_{150}}$ is the binding energy of the magnesium slab, E_{Ti} is the energy of a Ti atom, and $E_{\text{Mg–Ti}}$ is the Mg–Ti binding energy.

The clusterization energy in these two cases is –0.406 and –0.304 eV, respectively. The significant (about 0.1 eV) difference in the clusterization energies for structures with different locations of Ti atoms indicates the most probable formation of the state in which Ti atoms form a hexagonal lattice corresponding to the magnesium lattice.

Further, we simulated the increase in the number of Ti atoms on the Mg surface. The calculations were performed so that they revealed the optimal direction of growth of the Ti cluster (namely, its growth over the surface or the formation of step structures; see Fig. 6).

The Ti–Ti binding energy per atoms was calculated by the formula

$$E_{\text{Ti–Ti}} = \frac{1}{3}(E_{\text{Mg}_{150}\text{Ti}_{10}} - E_{\text{Mg}_{150}\text{Ti}_7} - 3E_{\text{Ti}}), \quad (5)$$

where $E_{\text{Mg}_{150}\text{Ti}_{10}}$ is the energy of the magnesium slab modified by ten Ti atoms, $E_{\text{Mg}_{150}\text{Ti}_7}$ is the energy of the magnesium slab modified by seven Ti atoms, and E_{Ti} is the energy of a single Ti atoms. The Ti–Ti binding energy is –4.763 eV in the former case and –5.893 eV

in the latter case. These data indicate that it is more advantageous for Ti atoms to form step clusters.

Next we studied the predissociation state of a hydrogen molecule on the surface of pure magnesium. For this purpose, it was placed above one of the Mg atoms in two different positions (along the Mg–Mg bond and across it; see Fig. 7).

As a result of the optimization procedure, the distance between the H_2 molecule and the magnesium surface increased by about 4 Å. The H–H spacing in this case was 0.74 Å, which corresponds to the equilibrium spacing in a hydrogen molecule, while the energy of this system corresponded to the sum of its individual components. This means that no predissociation state is observed for the given system, which indicates hampered dissociation of hydrogen on the surface of pure magnesium.

Analogously, we estimated the possibility of a predissociated state of a hydrogen molecule upon its addition to the surface of a cluster of seven Ti atoms located on the magnesium slab. For our analysis, we chose a cluster with the minimal number of atoms at the boundary since it possessed the minimal energy. Figure 8 shows the calculated structure of the most optimal position of the hydrogen molecule on the surface of the titanium cluster. In addition to this state, we also simulated other versions of the location of hydrogen; in particular, versions of its location above the central Ti atom, as well as various orientations of the adsorbed molecule relative to the Ti–Ti bonds. As a result of optimization of the geometry, the configuration of the predissociated state, in which hydrogen was above of one of the extreme atoms of the titanium cluster, was found to be most advantageous from the energy point of view. In this state, the distance between a Ti atom and the H_2 molecule was 1.9 Å, while the H–H spacing was 0.88 Å. The Ti–H binding energy per atom, amounting to –0.153 eV, was calculated by the formula

$$E_{\text{Ti–H}} = \frac{1}{2}(E_{\text{Mg}_{150}\text{Ti}_7\text{H}_2} - E_{\text{Mg}_{150}\text{Ti}_7} - E_{\text{H}_2}), \qquad (6)$$

where $E_{\text{Mg}_{150}\text{Ti}_7\text{H}_2}$ is the total binding energy of the system under investigation together with the hydrogen molecule at the surface, $E_{\text{Mg}_{150}\text{Ti}_7}$ is the energy of the magnesium slab together with the cluster of seven Ti atoms, and E_{H_2} is the binding energy of the hydrogen molecule.

The value of the Ti–H binding energy obtained here indicates that the existence of a predissociation state of a hydrogen molecule on the surface of a Mg slab covered by the Ti cluster is advantageous; consequently, hydrogen molecules dissociate on such a surface more easily.

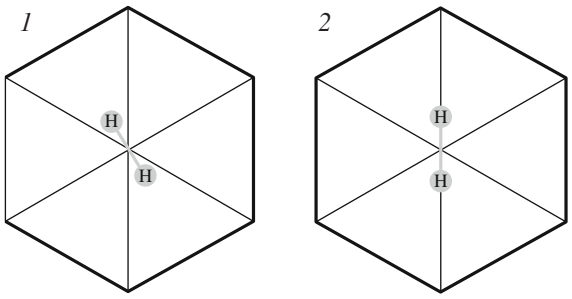

Fig. 7. Versions of arrangement of a hydrogen molecule on the (0001) surface of the magnesium slab: *1*—H_2 molecule is across the Mg–Mg bond; *2*—H_2 molecule is along the Mg–Mg bond.

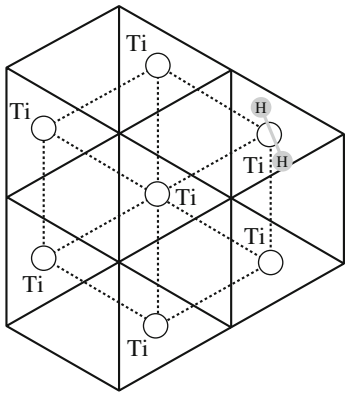

Fig. 8. Location of the H_2 molecule above one of the atoms of a titanium cluster located on the (0001) surface of a magnesium slab.

3. CONCLUSIONS

In the course of this study, we calculated the pressure in magnesium nanoparticles; it was found that for nanoparticles with a radius smaller than 5 nm, calculations can be carried out for periodic structures under zero pressure since the pressure n such nanoparticles is lower than 3 kbar. On the basis of these assumptions, we calculated a number of parameters of hydrogen sorption in the bulk and on the surface of magnesium as well as in $Mg_{53}Sc$ and $Mg_{53}Ti$ crystals. It was shown that the addition of titanium atoms to the magnesium structure lowers the potential barrier for jumps of hydrogen atoms between two nearest energy minima. This must sharply increase the hydrogen diffusion rate in magnesium hydrides. It was also established that titanium atoms form stable clusters on the magnesium surface, on which is formed a predissociation state of hydrogen facilitating diffusion of hydrogen atoms to the bulk of the crystal.

The results of our investigation suggest the possibility of using dilute alloys of magnesium with certain *d* metals as sorbents of hydrogen since these admixtures sharply accelerate diffusion of hydrogen atoms in the crystal lattice, as well as dissociation of hydrogen molecules on the magnesium surface. Titanium is a promising substituent of magnesium in the alloy.

ACKNOWLEDGMENTS

This study was supported financially by the Russian Foundation for Basic Research (project no. 06-02-16132). The authors are also grateful to the Institute of Computer Modeling of the Siberian Branch of the Russian Academy of Science for providing a cluster computer on which all quantum-chemistry calculations were performed.

REFERENCES

1. J. L. Slack, Sol. Energy Mater. Sol. Cells **90**, 485 (2006).
2. K. Higuchi, J. Alloys Compd. **330**, 526 (2002).
3. D. Kyoi, T. Sato, E. Ronnebro, et al., J. Alloys Compd. **372**, 213 (2004).
4. P. Hohenberg and W. Kohn, Phys. Rev. **136**, 864 (1964).
5. W. Kohn and L. J. Sham, Phys. Rev. **140**, 1133 (1965).
6. G. Kresse and J. Hafner, Phys. Rev. B: Condens. Matter **47**, 558 (1993).
7. G. Kresse and J. Hafner, Phys. Rev. B: Condens. Matter **49**, 14251 (1994).
8. G. Kresse and J. Furthmüller, Phys. Rev. B: Condens. Matter **54**, 11169 (1996).
9. D. Vanderbilt, Phys. Rev. B: Condens. Matter **41**, 7892 (1990).
10. S. Wei, Phys. Rev. B: Condens. Matter **50**, 4859 (1994).
11. G. Wulff, Z. Kristallogr. Mineral. **34**, 449 (1901).
12. C. Herring, Phys. Rev. **82**, 87 (1951).
13. P. Vajeeston, Phys. Rev. Lett. **89**, 175506 (2002).
14. G. Mills, H. Jonsson, and G. K. Schenter, Surf. Sci. **324**, 305 (1995).
15. G. Liang, J. Huot, S. Boilb, et al., J. Alloys Compd. **292**, 247 (1999).

Translated by N. Wadhwa